

Yu-fang LIU, Hong-sheng ZHAI, Ya-li GAO

# Product polarization distribution: Stereodynamics of the reaction of atom H and radical NH

© Higher Education Press and Springer-Verlag 2008

**Abstract** The product angular momentum polarization of the reaction of H+NH is calculated via the quasiclassical trajectory method (QCT) based on the extended London-Eyring-Polanyi-Sato (LEPS) potential energy surface (PES) at a collision energy of 5.1 kcal/mol. The calculated results of the vector correlations are denoted by using the angular distribution functions. The polarization-dependent differential cross sections (PDDCSs) demonstrate that the rotational angular momentum of the product H<sub>2</sub> is aligned and oriented along the direction perpendicular to the scattering plane. Vector correlation shows that the angular momentum of the product H<sub>2</sub> is aligned in the plane perpendicular to the velocity vector. It suggests that the reaction proceeds preferentially when the reactant velocity vector lies in a plane containing all three atoms. The orientation and alignment of the product angular momentum affects the scattering direction of the product molecules. The polarization-dependent differential cross sections (PDDCSs) reveal that scattering is predominantly in the backward hemisphere.

**Keywords** quasiclassical trajectory, differential cross sections, vector correlation

**PACS numbers** 34.20.Mq, 82.20.Fd, 82.20.Hf

## 1 Introduction

The reaction  $\text{H} + \text{NH} \rightarrow \text{N} + \text{H}_2$  is important mainly

Yu-fang LIU<sup>1</sup> (✉), Hong-sheng ZHAI<sup>1</sup>, Ya-li GAO<sup>1</sup>

<sup>1</sup> Department of Physics, Henan Normal University, Xinxiang 453007, China  
E-mail: yf-liu@henannu.edu.cn

Received December 13, 2007; accepted February 4, 2008

because of its impact on the processes that occur in the combustion of nitrogenous compounds [1]. The reaction of  $\text{NH}(X^3\Sigma^-) + \text{H}(^2S)$  has been studied in rich premixed  $\text{H}_2/\text{O}_2/\text{Ar}$  flames doped with  $\text{CH}_3\text{CH}$  in the temperature range  $1790 \text{ K} \leq T \leq 2200 \text{ K}$  [2]. The  $\text{NH}(X)$  concentration has been followed by laser-induced fluorescence (LIF). The rate of removal of  $\text{NH}(X)$  has been found to depend linearly on H atom concentration for a range of stoichiometries. *ab initio* study [3] of this reaction indicates that the reaction has a collinear transition state, and the barrier height is 1.69 kJ/mol. A recent study on the microdynamics of this reaction [4] illuminates that the reaction occurs via a direct channel and the product H<sub>2</sub> is mainly scattered backward. The product H<sub>2</sub> is in a cold excitation of its rotational state, but has a hot vibrational excitation. Kinetics of the reaction  $\text{H} + \text{NH} \leftrightarrow \text{N} + \text{H}_2$  have been studied using a direct *ab initio* dynamics method [5]. Thermal rate constants for this reaction were calculated using the microcanonical variational transition state theory. The calculated rate constants for both forward and reverse reactions are in good agreement with available experimental data. Pascual and co-workers [6] investigated the reaction on a global  $^4A''$  PES obtained from *ab initio* electronic structure calculations with the classical trajectories. Adam and Hack [7] presented a direct measurement of the rate coefficient of the reaction  $\text{NH}(X^3\Sigma^-) + \text{H}(^2S)$  at room temperature, calculated a PES for the  $^4A''$  state, and performed classical trajectory calculations for this reaction. On the other hand, the decomposition reaction  $\text{NH}_2(\tilde{X}) \rightarrow \text{NH}(X) + \text{H}(^2S)$  and the reverse reaction  $\text{N}(^4S) + \text{H}_2(X^1\Sigma_g^+) \rightarrow \text{NH}(X) + \text{H}(^2S)$  have been examined [8–12]. However, the vector correlation of this reaction has not been reported. To fully understand the

dynamics of an elementary reaction, it is important to study not only its scalar properties, but also its vector properties. Such properties, which include velocities and angular momentum, possess not only magnitudes that can be directly related to translational and rotational energies, but also well-defined directions. By understanding all the properties above, a complete picture of the scattering dynamics can be obtained.

Since the pioneering work of Fano and Macek [13] and of Herschbach and co-workers [14–17], it has been recognized that a detailed, three-dimensional picture of the dynamics of reactive collisions emerges with the determination of the correlated angular distribution describing mutual orientations of the reagent and product linear and angular momentum. Experimental and theoretical interest in vector correlation in the reaction processes  $A + BC \rightarrow AB + C$  has increased significantly in recent decades [18–28]. The most familiar vector correlation between the reagent and product relative velocity vector ( $k$ ,  $k'$ ) is characterized by the differential cross-section  $d\sigma/d\omega_t$ . Furthermore, the angular distribution describing the relative orientation of vectors  $k$ ,  $k'$ , and  $j'$  in space may be termed the  $k$ - $k'$ - $j'$  distribution (Fig. 1): The correlations which characterize it are some interesting double and triple vector correlations [29].

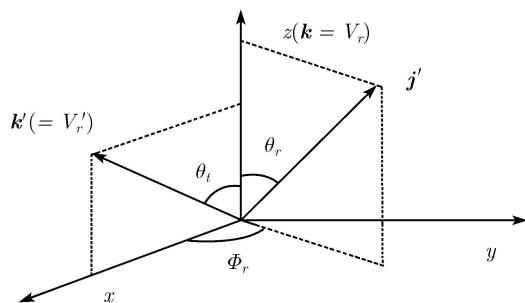


**Fig. 1** The center of mass coordinate system for describing the  $k$ ,  $k'$  and  $j'$  distribution.

The reaction  $H + NH \rightarrow N + H_2$  is a high-temperature reaction in the 2000–3000 K range. Quantum effects such as the tunneling and curvature effect are less important. It is suitable for the use of quasiclassical calculation to investigate the microdynamical characteristics of this reaction. The QCT method for the polarizations has been widely used in the homothetic reactions [30]. By using LEPS type PES of the collinear N–H–H, we calculate the minimal energy paths for this reaction and the product rovibrational distributions. In this research, we study the vector properties of this reaction by calculating the angle distribution functions  $P(\theta_r)$ ,  $P(\phi_r)$ ,  $P(\phi_r, \theta_r)$  and the polarization-dependent differential cross sections (PDDCSs).

## 2 Theory

### 2.1 Product distributions and vector correlations in the center-of-mass (CM) frame

The CM frame chosen has the  $z$ -axis parallel to the reagent relative velocity  $k$ , and the  $xz$ -plane contains  $k$  and  $k'$ . In the CM frame, the distribution of the angular momentum  $j'$  of the product molecule is described by the function  $f(\theta)$ , where  $\theta$  is the angle between  $j'$  and  $k$ .  $f(\theta)$  can be expanded in a Legendre polynomial series [31]:

$$f(\theta) = \sum a_n p_n(\cos \theta) \quad (1)$$

$n = 2$  indicates the product rotational alignment  $\langle P_2(j' \cdot k) \rangle = \langle 3 \cos^2 \theta \rangle / 2$ , where  $P_2$  is the second Legendre moment, and the brackets indicate an average over the distribution of  $j'$  about  $k$ . The  $k$ - $j'$  correlated CM angular distribution is written as the sum [31, 32]:

$$P(\omega_t, \omega_r) = \sum_{kq} \frac{[k]}{4\pi \sigma} \frac{1}{d\omega_t} \frac{d\sigma_{kq}}{d\omega_t} C_{kq}(\theta_r, \phi_r) \quad (2)$$

where  $(1/\sigma)(d\sigma_{kq}/d\omega_t)$  is the generalized polarization-dependent differential cross-section (PDDCS). The PDDCS is written in the following form:

$$\frac{1}{\sigma} \frac{d\sigma_{kq\pm}}{d\omega_t} = \frac{1}{4\pi} \sum_{k_1} [k_1] S_{kq\pm}^{k_1} C_{k_1-q}(\theta_t, 0) \quad (3)$$

where  $S_{kq\pm}^{k_1}$  is evaluated using the expected value expression:

$$S_{kq\pm}^{k_1} = \langle C_{k_1q}(\theta_t, 0) C_{kq}(\theta_r, 0) [(-1)^q e^{iq\phi_r} \pm e^{-iq\phi_r}] \rangle \quad (4)$$

where the angular brackets represent an average over all angles.

Many photoinitiated bimolecular reaction experiments will be sensitive only to polarization moments with  $k = 0$  and  $k = 2$ . To compare calculations with experiments,  $(2\pi/\sigma) (d\sigma_{00}/d\omega_t)$ ,  $(2\pi/\sigma) (d\sigma_{20}/d\omega_t)$ ,  $(2\pi/\sigma) (d\sigma_{22+}/d\omega_t)$  and  $(2\pi/\sigma) (d\sigma_{21-}/d\omega_t)$  are calculated. In the computation, PDDCSs are expanded up to  $k_1 = 7$ , which is sufficient for good convergence. The usual two vector correlations ( $k$ - $k'$ ,  $k$ - $j'$ ,  $k'-j'$ ) are expanded in a series of Legendre polynomials, and the distribution of the  $k$ - $j'$  correlation is characterized by  $P(\theta_r)$ . The  $P(\theta_r)$  can be written as [33, 34]:

$$P(\theta_r) = \frac{1}{2} \sum_k [k] a_0^k P_k(\cos \theta_r) \quad (5)$$

where the  $a_0^k$  coefficients (polarization parameters) are given by  $a_0^k = \langle P_k(\cos \theta_r) \rangle$  with the angular brackets

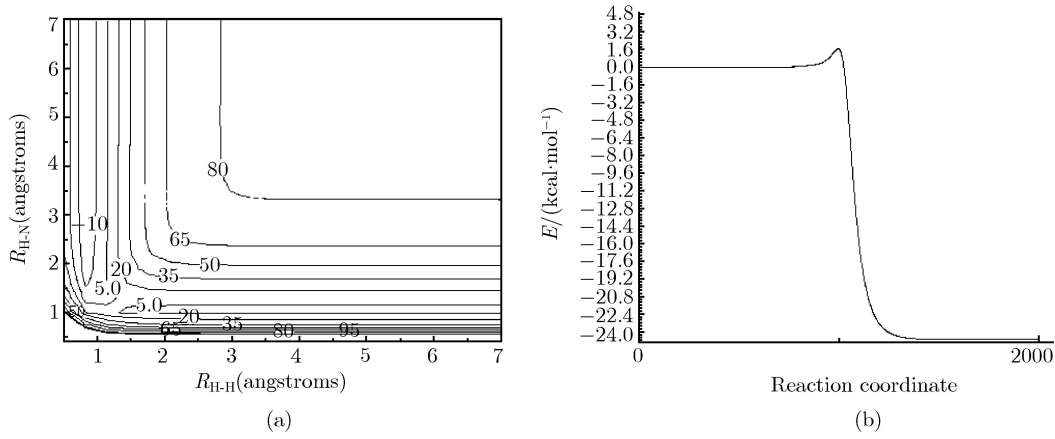


**Fig. 2** The contour of the LEPS-type PES for the reaction  $\text{H} + \text{NH}$  (a). It can be seen clearly that there is an “early” barrier in the reaction, but no well in the reaction channel. The energy as a function of the reaction path, traveling along the minimum energy path, is also shown in Fig. (b). The barrier height is 1.69 kcal/mol, which is in good agreement with the *ab initio* result [3] and the experimental value [10].

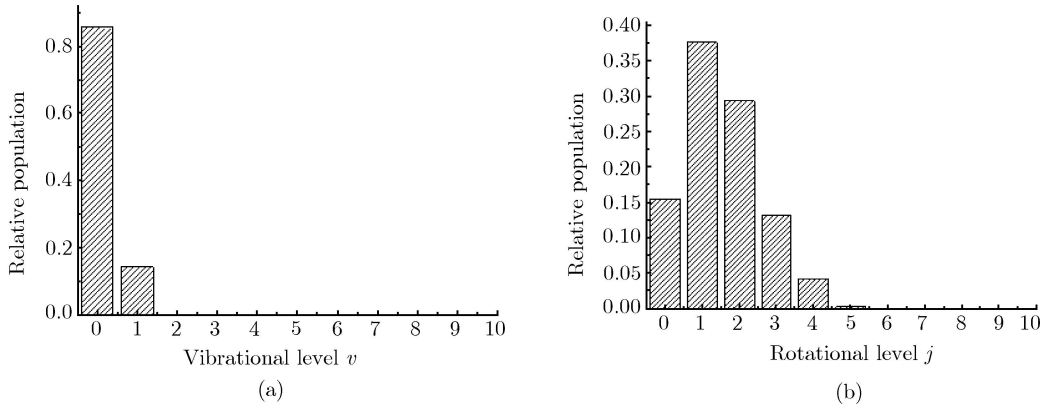


**Fig. 3** Ro-vibrational distributions of the product  $\text{H}_2$ . The product ro-vibrational distributions show that the produced  $\text{H}_2$  is cold, with the most probable vibrational quantum number  $v = 0$  and the most probable rotational quantum number  $j = 1$ . It is shown that most of the energies released from the reaction  $\text{H} + \text{NH}$  translates into the translational energy of the product  $\text{H}_2$ .

standing for an average over all the reactive trajectories. In this article, the  $P(\theta_r)$  is expanded up to  $k = 18$ , which shows a good convergence.

The dihedral angle distribution of the  $k$ - $k'$ - $j'$  correlation is characterized by the angle  $\phi_r$  [32, 35]. It has been shown that the distribution of dihedral angle  $\phi_r$  may be expanded as a Fourier series, and the  $\phi_r$  distribution can be written as:

$$P(\phi_r) = \frac{1}{2\pi} \left( 1 + \sum_{n_{\text{even}} \geq 2} a_n \cos n\phi_r + \sum_{n_{\text{odd}} \geq 1} b_n \sin n\phi_r \right) \quad (6)$$

with  $a_n$  and  $b_n$  yielding  $a_n = 2\langle \cos n\phi_r \rangle$ ,  $b_n = 2\langle \sin n\phi_r \rangle$ . In our computation,  $P(\phi_r)$  is expanded up to  $n = 24$  for a good convergence. The joint probability density function of angles  $\theta_r$  and  $\phi_r$ , which defines the direction of the angular momentum of the product ( $j'$ ), can be written as [35]:

$$\begin{aligned} P(\theta_r, \phi_r) &= \frac{1}{4\pi} \sum_{kq} [k] a_0^k C_{kq}(\theta_r, \phi_r)^* \\ &= \frac{1}{4\pi} \sum_k \sum_{q \geq 0} [a_{q\pm}^k \cos q\phi_r \\ &\quad - a_{q\mp}^k i \sin q\phi_r] C_{kq}(\theta_r, 0) \end{aligned} \quad (7)$$

The polarization parameter  $a_q^k$  is evaluated as:

$$a_{q\pm}^k = 2\langle C_{k|q}|(\theta_r, 0) \cos q\phi_r \rangle k, \quad \text{is even} \quad (8)$$

$$a_{q\mp}^k = 2i\langle C_{k|q}|(\theta_r, 0) \sin q\phi_r \rangle k, \quad \text{is odd} \quad (9)$$

In the calculation,  $P(\phi_r, \theta_r)$  is expanded up to  $k = 7$ , which is sufficient for good convergence.

## 2.2 Potential energy surface (PES) and quasiclassical trajectory calculations (QTC)

The extended London-Eyring-Polanyi-Sato (LEPS)

PES,

$$U(R_1, R_2, R_3) = Q_1 + Q_2 + Q_3 - \left\{ \frac{1}{2} [(J_1 - J_2) + (J_2 - J_3) + (J_3 - J_1)] \right\}^{1/2} \quad (10)$$

is employed in our calculations, where  $Q_i = ({}^1E_i + {}^3E_i)/2$ ,  $J_i = ({}^1E_i - {}^3E_i)/2$ . The  ${}^1E_i$  is defined as the diatomic Morse potential function, and the  ${}^3E_i$  is the anti-Morse function,

$${}^1E_i = D_i(\{1 - \exp[-\beta_i(r - r_0)]\}^2 - 1) \quad (11)$$

$${}^3E_i = {}^3D_i(\{1 + \exp[\beta_i(r - r_0)]\}^2 - 1) \quad (12)$$

where  ${}^3D_i = D_i(1 - S_i)/2(1 + S_i)$ .  $S_i$  is an adjustable parameter, while the subscript  $i = 1, 2, 3$  indicate H-H, H-N, H-N respectively.

In this paper, we use the 3-atom model quasiclassical trajectory method with a time step of 0.1 fs and integral time of 1000 fs. The accuracy of the trajectory is checked by the conservation of total energy and total angular momentum, and more critically by backward integration from the final state ( $t = t_f$ ) to the initial state ( $t = 0$ ). The initial state of NH is in its ground rotational and vibrational state and the initial collision energy is 5.1 cal/mol, corresponding to the Maxwell-Boltzma distribution at 2000 K. To obtain results with good statistics, 50 000 trajectories are calculated. The parameters of extended-LEPS PESs are presented in Table 1. Here, the Sato parameters are taken from Ref. [4].

**Table 1** Parameters used in the LEPS potential surface for the reaction H + NH.

Parameters	H-H	H-N	H-N
$\beta_e/\text{\AA}^{-1}$	1.94	1.58	1.58
$r_e/\text{\AA}$	0.0741	1.0360	1.0360
$D_e/(\text{kJ}\cdot\text{mol}^{-1})$	0.0741	1.0360	1.0360
Sato*	0.364	0.10	-0.10

\*Taken from Ref. [4].

### 3 Results and discussion

Vector correlation and the polarization-dependent, “generalized” differential cross-sections (PDDCS) for the reaction  $\text{H} + \text{NH} \rightarrow \text{N} + \text{H}_2$  are presented in Fig. 4. In Fig. 4 (a), the  $P(\theta_r)$  distribution has a peak at angle  $\theta_r$  which is close to  $\pi/2$  and symmetric with respect to  $\pi/2$ . The distribution of  $P(\theta_r)$ , which represents the  $k'-j'$  correlation, follows a cylindrical symmetry in the product scattering frame and has  $J_{\text{H}_2}$  always perpendicular to  $u_{\text{H}_2}$ . The dihedral angle distribution  $P(\phi_r)$  displayed in Fig. 4 (b) tends to be asymmetric with respect to the scattering

plane, directly reflecting the strong polarization of angular momentum. It indicates that the distribution of  $j'$  does not have azimuthal symmetry about the initial relative velocity vector of the H+NH reaction. In particular, the  $P(\phi_r)$  provides new insight into the reorienting or polarizing role played by the potential energy surface. The peak of the  $P(\phi_r)$  at  $\phi_r = \pi/2$  and  $\phi_r = 3\pi/2$  shows that most of the product molecules are ejected with  $j'$  aligning along the CM  $y$ -axis. This behavior suggests that the reaction proceeds preferentially when the reactant velocity vector lies in a plane containing all three atoms. However, given the very low probability of such planar collisions for an initially random orientation of reactant molecules, one must conclude that the potential energy surface reorients or polarizes the plane containing the three atoms into the  $k-k'$  plane during the reaction process. The peak of the  $P(\phi_r)$  at  $\phi_r = 3\pi/2$  is also apparently stronger than that at  $\phi_r = \pi/2$  for the reaction H+NH. The calculation results illustrate that the rotational angular momentum of the product  $\text{H}_2$  is not only aligned, but also oriented along the direction perpendicular to the scattering plane. Figure 4 (c) presents the angular momentum polarization in the form of polar plots in  $\theta_r$  and  $\phi_r$ , averaged over all scattering angles. It can be seen clearly that the distributions of  $P(\phi_r, \theta_r)$  peak at  $\phi_r = \pi/2$ ,  $\phi_r = 3\pi/2$ . This denotes the rotational angular momentum of the products perpendicular to the  $k-k'$  plane. The distributions of the  $P(\phi_r, \theta_r)$  are in good accordance with the distributions of  $P(\theta_r)$  and  $P(\phi_r)$ .

Figure 4 (d) displays the distribution of four PDDCS with the angle  $\theta_r$  between  $k$  and  $k'$  for the reaction H + NH. The PDDCSs describe the  $k-k'-j'$  correlation and the scattering direction of the product. The  $(2\pi/\sigma)(d\sigma_{00}/d\omega_t)$  pictures the  $k-k'$  correlation or the scattering direction of the product molecule. It can be seen from the distribution of  $(2\pi/\sigma)(d\sigma_{00}/d\omega_t)$  that the product molecules are mainly scattered backward. This is in agreement with the result of Ref. [4]. The  $(2\pi/\sigma)(d\sigma_{20}/d\omega_t)$ , whose value is the expectation value of the second Legendre moment, shows the trend which is opposite that of  $(2\pi/\sigma)(d\sigma_{00}/d\omega_t)$ , because the expected values  $\langle P_2(\cos\theta_r) \rangle$  are negative. When the reaction shows a strong alignment, the PDDCS for  $k = 0$ ,  $q \neq 0$  are shown in Fig. 4 (d). At the extremes of forward and backward scattering, the PDDCS with  $q \neq 0$  are necessarily zero. At these limiting scattering angles, the  $k-k'$  scattering plane is not determined and the value of these PDDCSs with  $q \neq 0$  must be zero. The PDDCS with  $q \neq 0$  at the scattering angles away from the extreme forward and backward directions provide information on the  $\phi_r$  dihedral angle distribution and are nonzero at

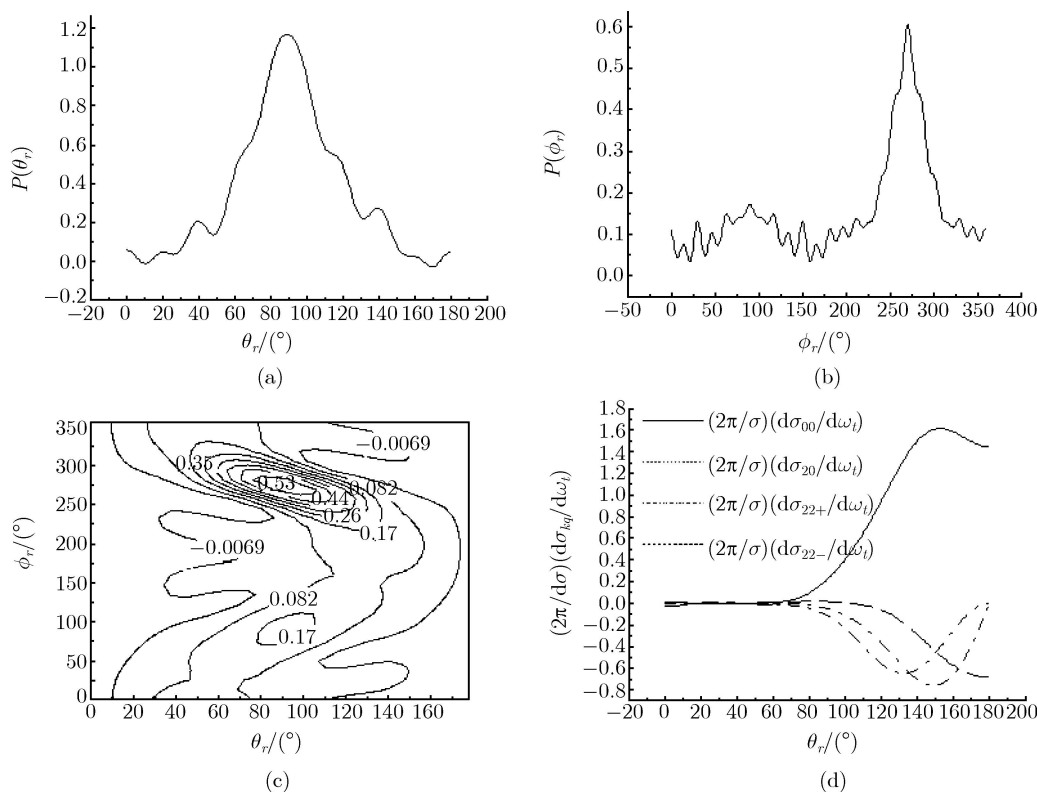


**Fig. 4** (a) The distribution of  $P(\theta_r)$ , reflecting the  $k'$ - $j'$  correlation. (b) The dihedral angular distribution of  $j'$ ,  $P(\phi_r)$  with respect to the  $k$ - $k'$  plane. (c) Polar plots of  $P(\theta_r, \phi_r)$  distribution averaged over all scattering angles. (d) Four PDDCS, solid line indicating  $(2\pi/\sigma)(d\sigma_{00}/d\omega_t)$ , dash indicating  $(2\pi/\sigma)(d\sigma_{20}/d\omega_t)$ , shot dash dot line indicating  $(2\pi/\sigma)(d\sigma_{22+}/d\omega_t)$ , dash dot line indicating  $(2\pi/\sigma)(d\sigma_{21-}/d\omega_t)$ .

scattering angles away from  $\theta_r = 0$  and  $\pi$ . This indicates that the  $P(\phi_r, \theta_r)$  distribution is not isotropic for sideway-scattering products.

## 4 Conclusion

This paper has presented a quasiclassical trajectory study of product polarization from the reaction  $\text{H} + \text{NH} \rightarrow \text{N} + \text{H}_2$ . We calculated the minimal energy paths for the reaction  $\text{H} + \text{NH}$ , the product ro-vibrational distributions, vector correlation and four polarization-dependent “generalized” differential cross sections (PDDCS). The calculated differential cross section  $(2\pi/\sigma)(d\sigma_{00}/d\omega_t)$  illustrates that the scattering is predominantly in the backward hemisphere. Vector correlation indicates that  $J_{\text{H}_2}$  is aligned in the plane perpendicular to the velocity vector, and the reaction proceeds preferentially when the reactant velocity vector lies in a plane containing all three atoms. The four PDDCSs give a good explanation about the vector correlation.

**Acknowledgements** This work was supported by the National Natural Science Foundation of China (Grant Nos. 10574039 and

10174019), the Foundation for Key Program of Ministry of Education of China (Grant No. 206084), the Henan Province Innovation Project for University Prominent Research Talents (HAIPUTT2006KYCX002), and the Innovation Scientists and Technicians Troop Construction Projects of Henan Province (Grant No. 084100510011).

## References

1. J. E. Dove and S. W. Nip, *Can. J. Chem.*, 1979, 57: 689
2. C. Morley, 18th Symp. Int. Combust., Pittsburgh, PA: The Combustion Institute, 1981, 18: 23
3. Z. F. Xu, D. C. Fang, and X. Y. Fu, *J. Phys. Chem.*, 1997, 101: 4432
4. L. J. Xu, J. M. Yan, and K. FA., *Chin. Sci. Bul.*, 1999, 44: 11
5. S. W. Zhang and T. N. Truong, *J. Chem. Phys.*, 2000, 113: 6149
6. R. Z. Pascual, G. C. Schatz, G. Lendvay, and D. Troya, *J. Phys. Chem. A*, 2002, 106: 4125
7. L. Adam, W. J. Hack, H. Zhu, Z. W. Qu, and R. Schinke, *J. Chem. Phys.*, 2005, 122: 114301
8. Ya Basevich and V. I. Vedeneev, *Khim. Fiz.*, 1988, 7: 1552
9. M. Koshi, M. Yoshimura, K. Fukuda, H. Matsui, K. Saito, M. Watanabe, A. Imamura, and C. J. Chen, *Chem. Phys.*,

- 1990, 93: 8703
10. F. Davidson and R. K. Hanson, *Int. J. Chem. Kinet.*, 1990, 22: 843
  11. N. Aleksandrov, V. Ya Basevich, and V. I. Vedeneev, *Khim. Fiz.*, 1994, 13: 90
  12. C. Ottinger, M. Brozis, and A. Kowalski, *Chem. Phys. Lett.*, 1999, 315: 355
  13. U. Fano and H. H. Macek, *Rev. Mod. Phys.*, 1973, 45: 553
  14. D. E. Case and D. R. Herschbach, *Mol. Phys.*, 1975, 30: 1537
  15. G. M. McClelland and D. R. Herschbach, *J. Phys. Chem.*, 1979, 83: 1445
  16. J. D. Barnwell, J. G. Loeser, and D. R. Herschbach, *J. Phys. Chem.*, 1983, 87: 2781
  17. G. M. McClelland and D. R. Herschbach, *J. Phys. Chem.*, 1987, 91: 5509
  18. M. L. Wang, K. L. Han, J. P. Zhan, V. W. K. Wu, G. Z. He, and N. Q. Lou, *Chem. Phys. Lett.*, 1997, 278: 307
  29. M. L. Wang, K. L. Han, and G. Z. He, *J. Chem. Phys.*, 1998, 109: 5446
  20. B. Soep and R. Vetter, *J. Phys. Chem.*, 1995, 99: 13569
  21. X. Zhang, T. X. Xie, M. Y. Zhao, and K. L. Han, *Chin. J. Chem. Phys.*, 2002, 15: 169
  22. B. Y. Chen Dating, K. L. Han, and N. Q. Lou, *Chin. J. Chem. Phys.*, 2002, 15: 247
  23. S. L. Cong, Y. M. Li, H. M. Yin, J. Sun, and K. L. Han, *Chin. J. Chem. Phys.*, 2002, 15:198
  24. J. Y. Liu, W. H. Fan, K. L. Han, D. L. Xu, and N. Q. Lou, *Chin. J. Chem. Phys.*, 2003, 16: 161
  25. M. L. Wang, K. L. Han, and G. Z. He, *J. Chem. Phys.*, 1998, 109: 5446
  26. K. L. Han, G. Z. He, and N. Q. Lou, *J. Chem. Phys.*, 1992, 96: 7865
  27. K. L. Han, G. Z. He, and N. Q. Lou, *Chem. Phys. Lett.*, 1992, 193: 165
  28. Y. F. Liu, Z. Z. Liu, G. S. Lv, L. J. Jiang, and J. F. Sun, *Chem. Phys. Lett.*, 2006, 423:157
  29. F. J. Aoiz, M. Brouard, and P. A. Enriquez, *J. Chem. Phys.*, 1996, 105: 4964
  30. M. D. Chen, K. L. Han, and N. Q. Lou, *Chem. Phys.*, 2002, 283: 463
  31. A. J. Orr-Ewing and R. N. Zare, *Annu. Rev. Phys. Chem.*, 1994, 45: 315
  32. M. Brouard, H. M. Lambert, S. P. Rayner, and J. P. Simpson, *Mol. Phys.*, 1996, 89: 403
  33. F. J. Aoiz, M. Brouard, and P. A. Enriquez, *J. Chem. Phys.*, 1996, 105: 4964
  34. F. J. Aoiz, M. Brouard, V. J. Herrero, V. S. Rabanos, and K. Stark, *Chem. Phys. Lett.*, 1997, 64: 487
  35. A. J. Alexander, F. J. Aoiz, L. Banareas, M. Brouard, J. Short, and J. P. Simons, *J. Phys. Chem. A*, 1997, 101: 7544